ANTIMICROBIAL AGENTS AND CHEMOTHERAPY, Jan. 2008, p. 98–109 Vol. 52, No. 1
0066-4804/08/$08.00+0 doi:10.1128/AAC.00609-07

Artemisinin and a Series of Novel Endoperoxide Antimalarials Exert Early Effects on Digestive Vacuole Morphology▽‡

Maria del Pilar Crespo,[1]† Thomas D. Avery,[2]† Eric Hanssen,[1,3] Emma Fox,[1] Tony V. Robinson,[2] Peter Valente,[2] Dennis K. Taylor,[2] and Leann Tilley[1,3]*

Department of Biochemistry[1] and ARC Centre of Excellence for Coherent X-ray Science,[3] La Trobe University, Melbourne, Victoria 3086, Australia, and Department of Chemistry, Adelaide University, Adelaide, South Australia 5005, Australia[2]

Received 8 May 2007/Returned for modification 9 July 2007/Accepted 9 September 2007

Artermisinin and its derivatives are now the mainstays of antimalarial treatment; however, their mechanism of action is only poorly understood. We report on the synthesis of a novel series of epoxy-endoperoxides that can be prepared in high yields from simple starting materials. Endoperoxides that are disubstituted with alkyl or benzyl side chains show efficient inhibition of the growth of both chloroquine-sensitive and -resistant strains of *Plasmodium falciparum*. A *trans*-epoxide with respect to the peroxide linkage increases the activity compared to that of its *cis*-epoxy counterpart or the parent endoperoxide. The novel endoperoxides do not show a strong interaction with artemisinin. We have compared the mechanism of action of the novel endoperoxides with that of artemisinin. Electron microscopy reveals that the novel endoperoxides cause the early accumulation of endocytic vesicles, while artemisinin causes the disruption of the digestive vacuole membrane. At longer incubation times artemisinin causes extensive loss of organellar structures, while the novel endoperoxides cause myelin body formation as well as the accumulation of endocytic vesicles. An early event following endoperoxide treatment is the redistribution of the pH-sensitive probe LysoSensor Blue from the digestive vacuole to punctate structures. By contrast, neither artemisinin nor the novel endoperoxides caused alterations in the morphology of the endoplasmic reticulum nor showed antagonistic antimalarial activity when they were used with thapsigargin. Analysis of rhodamine 123 uptake by *P. falciparum* suggests that disruption of the mitochondrial membrane potential occurs as a downstream effect rather than as an initiator of parasite killing. The data suggest that the digestive vacuole is an important initial site of endoperoxide antimalarial activity.

Artemisinin is a sesquiterpene lactone antimalarial with a 1,2,4-trioxane heterocyclic core that incorporates a peroxide linkage that is essential for its activity (44). Artemisinin is of major importance as a frontline treatment for malaria, particularly as it is active against chloroquine (CQ)-resistant strains of *Plasmodium falciparum* (20, 23, 24, 45, 66, 74). Several groups have reported on pathways for the synthesis of artemisinin, but all require numerous steps and have low yields (5, 35). As a result, artemisinin-based antimalarials are produced semisynthetically from extracts of *Artemisia annua*. A period of over 1 year is needed for the horticultural, harvesting, extraction, and manufacturing processes (34, 41, 45), which limits the ease of scale-up of production and makes artemisinin derivatives much more expensive than traditional antimalarials, such as CQ and sulfadoxine-pyrimethamine. Indeed, artemisinin combinations are too costly for many patients, and the supply of counterfeit or inferior drugs is a major problem (4, 45, 71). Another issue is the fact that artemisinin and its derivatives are not suitable for prophylaxis or for use as a monotherapy due to their very short half-lives in vivo. These factors have been the driving force behind a large number of analogue syntheses (52, 65). However only 10 structural classes of synthetic endoperoxides are currently under investigation (26), which is rather few, given that artemisinin derivatives are effectively the only drugs left in our antimalarial armory.

Recently, Vennerstrom et al. reported on the synthesis of a new synthetic peroxide antimalarial called OZ277 (70). OZ277 contains a five-membered 1,2,4-trioxolane, more commonly known as a secondary ozonide, that is amenable to large-scale synthesis. OZ277 has pharmacokinetic properties that are superior to those of artemisinin derivatives; however, its half-life is still only about 2 h (40, 51). OZ277 has recently been subjected to phase II trials (70) but apparently showed a poor half-life in vivo and is no longer supported by the Medicines for Malaria Venture (43). This setback, coupled with the inevitable development of resistance to any antimalarial that is employed in the field, makes it important to continue the development of novel endoperoxides, especially compounds with potentially longer half-lives or different molecular targets.

We have developed a simple synthetic pathway for the preparation of a novel series of epoxy-endoperoxides (65). The epoxide and endoperoxide moieties are designed to mimic the oxygen atom arrangement in artemisinin, and we have previously generated compounds with considerable antimalarial activity (65). In an effort to improve on the antimalarial activity of this series, we have now investigated the epoxides of a series of bicyclic endoperoxides in which the carbons adjacent to the peroxide linkage are tetrasubstituted. This substitution is known to increase the lifetime of the alkoxy radicals generated upon homolytic cleavage of the peroxide unit (48) over cases in which the substituent is H (65) or OH (53). Indeed, it is well

* Corresponding author. Mailing address: Department of Biochemistry, La Trobe University, Plent Rd., Melbourne, 3086 Victoria, Australia. Phone: 61-3-94791375. Fax: 61-3-94792467. E-mail: L.Tilley@latrobe.edu.au.

† These authors contributed equally to this work.

‡ Supplemental material for this article may be found at http://aac.asm.org/.

▽ Published ahead of print on 15 October 2007.

known that metal (Fe)-induced cleavage of the peroxide linkage to initially form alkoxy radicals followed by β-scission to form downstream carbon radicals is key to the activity of artemisinin (59, 70). Thus, peroxide analogues with hydrogen atoms on the carbons adjacent to the peroxide linkage will not have the same propensity to form damaging carbon radicals downstream, as intramolecular hydrogen atom abstraction will be dominant in these cases, quenching the oxygen-centered radicals formed by peroxide bond cleavage (6, 22).

We have determined the antimalarial parasite activities of the novel epoxy-endoperoxides and investigated their mechanisms of action. Active endoperoxide antimalarials are assumed to interact with reduced heme (ferroprotoporphyrin IX) or iron to form free-radical products of both the drug and the heme (27, 43, 49, 52, 60). The radicals are thought to react with susceptible groups within parasite enzymes and lipids (10, 11, 37, 44, 47, 55, 56); however, the exact site of action is still a matter of debate.

A recent report implicates the *P. falciparum* homologue of the sarco/endoplasmic reticulum (ER) Ca^{2+} ATPase (SERCA) as a major downstream target of activated artemisinin in the parasite cytoplasm (15); however, the synthetic endoperoxide OZ277 inhibits SERCA much less potently (69). In *Saccharomyces cerevisiae*, components of the mitochondrial electron transport chain have also been shown to be susceptible to artemisinin (36); however, it has not been demonstrated if these are important targets in plasmodia. In this work we have examined the effects of artemisinin and the most active of the novel endoperoxide antimalarials on the morphology of the parasite's mitochondrion, ER, and digestive vacuole. We conclude that disruption of the digestive vacuole function is an early event in the action of endoperoxide antimalarials.

MATERIALS AND METHODS

Parasites and assessment of antimalarial activity. D10 and 3D7 are CQ-sensitive strains of *P. falciparum*, and K1 is a CQ-resistant strain of *P. falciparum* (17, 19). *P. falciparum*-infected erythrocytes (RBCs) were cultured in medium containing 4% human serum and 0.5% GIBCO AlbuMAX I (Invitrogen) in RPMI 1640 supplemented with hypoxanthine and glutamate, as described previously (18), by using blood donated by the Red Cross Blood Service, Melbourne, Australia. The parasites were plated at about a 1% parasitemia (2% hematocrit) in 96-well trays, and different concentrations of the compounds were added as serial dilutions in hypoxanthine-free medium from concentrated stocks in methanol or dimethyl sulfoxide. The final solvent concentration was less than 0.1%. The parasites were incubated for 48 h, with daily replacement of the drug-supplemented medium. Growth curves based on the uptake of [^{3}H]hypoxanthine were obtained in triplicate, as described previously (58), and the concentration of compound required to produce 50% inhibition of growth (IC_{50}) was determined.

Drug interactions were assessed by isobologram analysis (1, 7, 12). Briefly, four different combinations of artemisinin or the novel endoperoxides (compounds 3a and 3c) with each other or with thapsigargin (a SERCA inhibitor) were serially diluted at a fixed ratio, and their effects on parasite growth (strain D10 or 3D7; 1% parasitemia) were examined. The IC_{50} values were calculated for each drug as though it had been added in isolation. These "apparent" IC_{50} values were divided by the IC_{50} values for the drugs used alone to determine the fractional inhibitory concentration (FIC). The FIC values for the two drugs used in the combination were added to give the sums of the FIC values (SFICs). The experiments were performed in duplicate on 2 or 3 days.

Electron microscopy. Ring-stage parasite-infected RBCs (strain D10 or 3D7) were incubated without drug or were treated with artemisinin or the novel endoperoxides (compounds 3a and 3c) at twice their respective IC_{50} values for 24 h. Alternatively, trophozoite-stage parasites were treated with 40 times the IC_{50} values for 4 or 8 h. The parasites were harvested at the trophozoite stage by floatation on a Percoll cushion (3), washed, and fixed in 0.1 M sodium cacodylate, pH 7.4, containing 1% glutaraldehyde and 0.5% paraformaldehyde for 18 h. The cells were rinsed and pelleted at 1,650 × *g* before being postfixed for 1 h with 1% osmium tetroxide. After the cells were washed, they were stained en block with 2% aqueous uranyl acetate and further rinsed before serial dehydration and embedding in LR-White. In some cases the cells were embedded in 10% gelatin and refixed with 2.5% glutaraldehyde in 0.1 M sodium cacodylate prior to dehydration. Sections (70 nm) were prepared, recovered on 200-mesh Formvar-coated copper grids, and then stained with aqueous uranyl acetate and lead citrate for examination at 80 kV on a Jeol 2010HC transmission electron microscope.

Digestive vacuole integrity. The pH-sensitive probe LysoSensor Blue-DND192 (Molecular Probes) was used to visualize acidic compartments. Trophozoite-stage parasite-infected RBCs (strain 3D7) were incubated without drug or were treated with artemisinin, compound 3a, or compound 3c at 2, 20, or 40 times their respective IC_{50} values for 4 or 8 h. The parasitized RBCs were resuspended in complete medium (3% hematocrit) and incubated with the pH-sensitive probe LysoSensor Blue (1 μM) at 37°C for 20 min. The parasitized RBCs were mounted wet on a glass slide, covered with a glass coverslip, and imaged within 20 min at ambient temperature (maintained at 20°C) by using an Olympus IX81 inverted microscope with DAPI filter settings. Three hundred infected RBCs were classified according to whether their digestive vacuole morphology was "normal" or "redistributed."

ER morphology. Trophozoite-stage parasite-infected RBCs (strain D10) were incubated without drug or were treated with thapsigargin, artemisinin, compound 3a, or compound 3c at 10 times their respective IC_{50} values for 12 h. Cultures were incubated with 500 nM ER Tracker Blue-White DPX probe for 30 min at 37°C. The cells were resuspended in fresh complete medium, and the ER fluorescence pattern was examined with a DAPI filter set. Three hundred infected RBCs were classified according to whether their ER morphology was "normal" or "condensed."

Mitochondrial integrity. Ring-stage parasite-infected RBCs (strain D10) were incubated without drug or were treated with artemisinin, compound 3a, or compound 3c at 2, 20, or 40 times their respective IC_{50} values for 24 h. Alternatively, trophozoite-stage parasites were treated for 4 h. As a control, samples of untreated parasites were incubated with the ionophores nigericin and monensin (20 μM each) to collapse the membrane potential. An aliquot of rhodamine 123 (final concentration, 0.2 μM) was added for 30 min at 37°C; and then the infected RBCs were washed three times in HEPES-buffered saline, resuspended in complete medium, and imaged with a Leica SP2 confocal microscope or an Olympus BX81 microscope with a ×100 oil immersion lenses (1.4 numerical aperture) and fluorescein settings. One thousand infected RBCs were classified as normal or rhodamine 123 depleted.

General synthetic methods. Solvents were dried by appropriate methods wherever needed. Thin-layer chromatography (TLC) used aluminum sheets (40 by 80 mm) were coated with silica gel 60 F_{254}, and the gels were visualized under 254-nm light or were developed in vanillin or permanganate dip. Flash chromatography was conducted with silica gel 60 with particle sizes of 0.040 to 0.063 mm. Melting points (Mps) were uncorrected. ^{1}H nuclear magnetic resonance (NMR) and ^{13}C NMR spectra were recorded in $CDCl_3$ solution at either 300 MHz or 600 MHz, and tetramethylsilane (0 ppm) and $CDCl_3$ (77.0 ppm) were used as internal standards. All yields reported refer to isolated material judged to be homogeneous by TLC and NMR spectroscopy.

1,4-Di-(3-methylphenyl)-1,3-cyclohexadiene (diene 1b). Diene 1b was synthesized by the general procedure outlined by Posner et al. (54). Mp, 99 to 101°C; ^{1}H NMR (300 MHz, $CDCl_3$) δ 2.37 (s, 6H), 2.76 (s, 4H), 6.51 (s, 2H), 7.00 to 7.40 (m, 8H); ^{13}C NMR (75 MHz, $CDCl_3$) δ 21.4, 26.1, 121.6, 122.1, 125.7, 127.9, 128.4, 136.0, 138.8, 140.8.

1-Bromo-4-fluorobenzene. To a two-necked round-bottom flask equipped with a condenser and a dropping funnel were added fluorobenzene (5 g; 52 mmol) and $FeCl_3$ (100 mg). The mixture was cooled to −8°C with an ice-salt bath. Bromine (8.5 g; 53 mmol) was then added dropwise over 2 h. Following addition of bromine, the reaction mixture was heated to 60°C for 1 h. The crude product was distilled at atmospheric pressure to yield 1-bromo-4-fluorobenzene (6.37 g, 70%) as a colorless oil. Boiling point, 148 to 152°C (150°C in the literature [J. Oren, 12 March 1997, European patent application EP 761627]).

4-Fluorophenyllithium. To a stirred solution of butyllithium (16 ml; 1.9 M in hexane) in dry diethyl ether (20 ml) under anhydrous nitrogen at −30°C was added dropwise 1-bromo-4-fluorobenzene (5.25 g, 30 mmol) in dry diethyl ether (20 ml). After addition, the reaction mixture was allowed to warm to room temperature. The product was used without further purification.

1,4-Di-(4-fluorophenyl)-1,4-cyclohexadiol. To a solution of 4-fluorophenyllithium in diethyl ether (40 ml; 30 mmol) was added a solution of 1,4-cyclohexanedione (0.84 g; 7.5 mmol) in diethyl ether (30 ml) over 30 min. The reaction mixture was brought to reflux for 30 min and cooled in an ice bath, and 10%

hydrochloric acid (100 ml) was added. The organic layer was separated, and the aqueous layer was extracted with ethyl acetate. The combined organics were dried ($MgSO_4$) and filtered, and the solvent was removed in vacuo. The crude product was purified by flash chromatography to yield 1,4-di-(4-fluorophenyl)-1,4-cyclohexadiol (1.25 g; 55%) as a colorless solid; R_f, 0.6 (2:3 ethyl acetate-hexane); ^{1}H NMR (300 MHz, $CDCl_3$) δ 1.55 (brs, 2OH), 1.69 to 1.82 (m, 4H), 2.31 to 2.45 (m, 4H), 7.08 to 7.03 (m, 4H), 7.57 to 7.53.

1,4-Di-(4-fluorophenyl)-1,3-cyclohexadiene and 1,4-di-(4-fluorophenyl)-1,4-cyclohexadiene (isomer mixture). To a solution of 1,4-di-(4-fluorophenyl)-1,4-cyclohexadiol (1.1 g; 3.6 mmol) in benzene (50 ml) was added *p*-toluenesulfonic acid (20 mg). The resulting reaction mixture was refluxed for 15 min, while the water that formed was removed by azeotropic distillation. The crystalline product that formed on cooling was recrystallized from ethanol to give a mixture of the 1,3- and 1,4-di-(4-fluorophenyl)-1,3-cyclohexadiene (70:30) (0.84 mg; 87%) as a yellow solid (G. H. Posner, 30 September 1997, U.S. patent application 5,672,624).

1,4-Di-(4-fluorophenyl)-1,3-cyclohexadiene (compound 1c). The isomeric mixture of 1,3- and 1,4-di-(4-fluorophenyl)-1,3-cyclohexadiene (0.2 g) was refluxed for 4 h in *t*-butanol (50 ml) containing potassium *t*-butoxide (1.4 g). After the mixture was cooled to room temperature, most of the *t*-butanol was removed and water (30 ml) was added. The mixture was extracted with diethyl ether, dried ($MgSO_4$), and filtered; and the solvent was removed in vacuo. The crude product was recrystallized from benzene to yield 1,4-di-(4-fluorophenyl)-1,3-cyclohexadiene (compound 1c; 0.19 g; 95%) as a pale yellow solid; ^{1}H NMR (300 MHz, $CDCl_3$) δ 2.75 (s, 4H), 6.44 (s, 2H), 7.08 to 7.01 (m, 4H), 7.45 to 7.42 (m, 4H) (Posner, U.S. patent application 5,672,624).

Methyl 3-(4-methylcyclohexa-1,3-dienyl)propanoate (compound 1d). A solution of 3-(4-methylcyclohexa-1,4-dienyl)propionic acid (1.833 g, 11.03 mmol) (13) in methanol (30 ml) and concentrated H_2SO_4 (1 ml) was refluxed overnight. The majority of the methanol was then removed in vacuo, and ether (50 ml) was then added and extracted with concentrated $NaHCO_3$ solution. The organic compounds were then dried ($MgSO_4$) and filtered, and the volatile compounds were removed in vacuo to give a crude mixture of 1,3- and 1,4-dienes. The diene mixture was then purified by column chromatography to give a mixture of methyl 3-(4-methylcyclohexa-1,3-dienyl)propanoate (compound 1d) and methyl 3-(4-methylcyclohexa-1,4-dienyl)propanoate (60:40) (1.039 g; 52%) as a colorless oil; R_f, 0.5 (1:9 ethyl acetate-hexane).

Methyl 3-(4-methylcyclohexa-1,3-dienyl)propanoate (compound 1d). ^{1}H NMR (300 MHz, $CDCl_3$) δ 1.76 (s, 3H), 2.11 (bs, 4H), 2.35 to 2.49 (m, 4H), 3.67 (s, 3H), 5.59 (bs, 2H).

Methyl 3-(4-methylcyclohexa-1,4-dienyl)propanoate. ^{1}H NMR (300 MHz, $CDCl_3$) δ 1.67 (s, 3H), 2.27 to 2.32 (m, 2H), 2.42 to 2.48 (m, 2H), 2.58 (bs, 4H), 3.67 (s, 3H), 5.40 (bs, 1H), 5.44 (bs, 1H).

General procedure for the synthesis of endoperoxides (42). A solution of the appropriate 1,3-butadiene (~4 g) in CH_2Cl_2 (30 ml/g) was photolyzed with three 500-W halogen lamps in the presence of Rose Bengal bis(triethylammonium) salt (100 mg) and oxygen for 6 h. The reaction was performed in a flask fitted with an external cooling jacket, and the temperature was maintained at below 5°C for the duration of the reaction. The solution was concentrated in vacuo, and the resulting residue was purified by flash chromatography.

1,4-Di-(3-methylphenyl)-2,3-dioxabicyclo[2.2.2]oct-5-ene (compound 2b). Yield, 0.47 g (21%); colorless solid; Mp, 99 to 101°C (hexane-dichloromethane); R_f, 0.38 (1:9 ethyl acetate-hexane); ^{1}H NMR (300 MHz, $CDCl_3$) δ 1.92 to 2.09 (m, 2H), 2.39 (s, 6H), 2.57 to 2.71 (m, 2H), 6.86 (s, 2H), 7.17 to 7.19 (m, 2H), 7.26 to 7.36 (m, 6H); ^{13}C NMR (75 MHz, $CDCl_3$) δ 21.5, 29.4, 78.3, 123.1, 127.0, 128.4, 129.2, 136.6, 138.3, 139.4; infrared (IR; Nujol) 1608, 1587, 1077, 931 cm^{-1}; mass spectrum (MS) *m/z* (with electron ionization [+EI]) 292 (M^+, 11), 260 (+EI, 100), 160 (+EI, 13), 119 (+EI, 33); high-resolution mass spectrometry (HRMS) (+EI) $(M + Na)^+$ found, 315.1359; $(M + Na)^+$ calculated for $C_{20}H_{20}O_2Na$, 315.1361.

1,4-Di-(4-fluorophenyl)-2,3-dioxa-bicyclo[2.2.2]oct-5-ene (compound 2c) (54). Yield, 51%; white solid; Mp, 152 to 153°C; R_f, 0.57 (1:4 ethyl acetate-hexane); ^{1}H NMR (300 MHz) δ 1.92 to 2.28 (m, 2H), 2.55 to 2.71 (m, 2H), 6.84 (s, 2H), 7.18 to 7.08 (m, 4H), 7.54 to 7.50 (m, 4H).

Methyl 3-(4-methyl-2,3-dioxa-bicyclo[2.2.2]oct-5-en-1-yl)propanoate (compound 2d). Yield, 411 mg (93%); colorless oil; R_f, 0.28 (1:4 ethyl acetate-hexane); ^{1}H NMR (300 MHz, $CDCl_3$) δ 1.38 (s, 3H), 1.44 to 1.60 (m, 2H), 1.98 to 2.17 (m, 4H), 2.39 to 2.57 (m, 2H), 3.69 (s, 3H), 6.42 (s, 2H); ^{13}C NMR (75 MHz, $CDCl_3$) δ 21.3, 28.15, 28.20, 29.5, 30.2, 51.7, 74.8, 76.2, 133.8, 136.6, 173.5; IR (neat) 1737, 1637, 1438, 1378, 1197, 1172, 883 cm^{-1}; MS *m/z* (+EI) 212 (M^+, <1), 211 (+EI, 3), 196 (+EI, 9), 181 (+EI, 100), 148 (+EI, 38), 123 (+EI, 67), 106 (+EI, 54); HRMS (+EI) $(M + Na)^+$ found, 235.0948; $(M + Na)^+$ calculated for $C_{11}H_{16}O_4Na$, 235.0946.

General procedure for the synthesis of epoxy-endoperoxides (21). To a solution of endoperoxide 2b (1 equivalent in CH_2Cl_2 [20 ml/g]) was added 70% *m*-chloroperbenzoic acid (2 equivalents), and the reaction mixture was stirred at ambient temperature until it was complete by TLC. Dichloromethane was then added and the solution was extracted with saturated $Na_2S_2O_3$, followed by extraction with saturated $NaHCO_3$. The organic layer was dried over $MgSO_4$ and filtered, and the volatile compounds were removed in vacuo. The crude epoxides were purified by column chromatography.

(±)(1*S*,2*R*,4*R*,5*S*)1,5-Di-(3-methylphenyl)-3,6,7-trioxatricyclo[3.2.2.02,4]nonane (compound 3b). The first isomer was the major product. Yield, 312 mg (59%); colorless solid; Mp, 143 to 145°C (hexane-dichloromethane); R_f, 0.38 (1:9 ethyl acetate-hexane); ^{1}H NMR (600 MHz, $CDCl_3$) δ 2.09 to 2.14 (m, 2H), 2.23 to 2.25 (m, 2H), 2.39 (s, 6H), 7.17 to 7.18 (m, 2H), 7.30 to 7.33 (m, 6H); ^{13}C NMR (75 MHz, $CDCl_3$) δ 21.5, 30.3, 54.9, 82.3, 122.1, 125.8, 128.6, 129.2, 138.4, 139.6; IR (Nujol) 1607, 1588, 890, 879, 784 cm^{-1}; MS *m/z* (+EI) 308 (M^+, 12), 291 (+EI, 11), 276 (+EI, 36), 248 (+EI, 34), 119 (+EI, 66), 91 (+EI, 100), 65 (+EI, 53); HRMS (+EI) $(M + Na)^+$ found, 331.1305; $(M + Na)^+$ calculated for $C_{20}H_{20}O_3Na$, 331.1310.

(±)(1*S*,2*S*,4*R*,5*R*)1,5-Di-(3-methylphenyl)-3,6,7-trioxatricyclo[3.2.2.02,4]nonane (compound 4b). The second isomer was the minor product. Yield, 141 mg (27%); colorless solid; Mp, 143 to 145°C (hexane-dichloromethane); R_f, 0.13 (1:9 ethyl acetate-hexane); ^{1}H NMR (300 MHz, $CDCl_3$) δ 2.22 to 2.34 (m, 2H), 2.39 (s, 6H), 2.68 to 2.86 (m, 2H), 3.68 (s, 2H), 7.22 to 7.36 (m, 6H), 7.44 (brs, 2H); ^{13}C NMR (75 MHz, $CDCl_3$) δ 21.4, 26.8, 54.3, 77.2, 123.6, 127.8, 128.6, 130.0, 137.0, 138.5; IR (Nujol) 1607, 1588, 881, 786 cm^{-1}; MS *m/z* (+EI) 308 (M^+, 3), 276 (+EI, 70), 248 (+EI, 28), 119 (+EI, 100), 91 (+EI, 21), 65 (+EI, 50); HRMS (+EI) $(M + Na)^+$ found, 331.1310; $(M + Na)^+$ calculated for $C_{20}H_{20}O_3Na$, 331.1310.

(±)(1*S*,2*R*,4*R*,5*S*)1,5-Di-(4-fluorophenyl)-3,6,7-trioxatricyclo[3.2.2.02,4]nonane (compound 3c). The first isomer was the major product. Yield, 77 mg (36%); pale yellow solid; Mp, 142 to 144°C (benzene); R_f, 0.65 (benzene); ^{1}H NMR (300 MHz, $CDCl_3$) δ 2.09 to 2.25 (m, 4H), 3.82 (s, 2H), 7.09 to 7.14 (m, 2H), 7.46 to 7.50 (m, 2H); ^{13}C NMR (75 MHz, $CDCl_3$) 30.2, 55.0, 82.2, 115.8, 116.1, 127.3, 127.4, 135.3, 135.4, 161.3, 165.4; IR (solid) 1610, 1508, 1232, 1225, 1159, 823 cm^{-1}; MS *m/z* (+EI) 316 (M^+, <1), 282 (+EI, 16), 271 (+EI, 15), 167 (+EI, 25), 123 (+EI, 100), 109 (+EI, 17), 95 (+EI, 25); HRMS (+EI) $(M + H)^+$ found, 317.0996; $(M + H)^+$ calculated for $C_{18}H_{15}F_2O_3$, 317.0989.

(±)(1*S*,2*S*,4*R*,5*R*)1,5-Di-(4-fluorophenyl)-3,6,7-trioxatricyclo[3.2.2.02,4]nonane (compound 4c). The second isomer was the minor product. Yield, 41 mg (19%); pale yellow solid; R_f, 0.22 (benzene); ^{1}H NMR (300 MHz, $CDCl_3$) δ 2.24 to 2.41 (m, 2H), 2.69 to 2.86 (m, 2H), 3.68 (s, 2H), 7.10 to 7.17 (m, 2H), 7.56 to 7.60 (m, 2H); ^{13}C NMR (75 MHz, $CDCl_3$) 27.1, 54.3, 77.1, 115.9, 116.2, 129.1, 129.2, 132.8, 160.8, 165.1; IR (solid) 1759, 1686, 1598, 1504, 1224, 1159, 841, 833 cm^{-1}; MS *m/z* (+EI) 316 (M^+, <1), 282 (+EI, 12), 266 (+EI, 13), 167 (+EI, 25), 123 (+EI, 100), 109 (+EI, 17), 95 (+EI, 25); HRMS (+EI) $(M + Na)^+$ found, 339.0808; $(M+Na)^+$ calculated for $C_{18}H_{14}F_2O_3Na$, 339.0809.

(±)(1*R*,2*S*,4*R*,5*R*)Methyl 3-(5-methyl-3,6,7-trioxatricyclo[3.2.2.02,4]nonane)propanoate (compound 3d). The first isomer was the minor product. Yield, 103 mg (39%); colorless oil; R_f, 0.45 (3:7 ethyl acetate-hexane); ^{1}H NMR (300 MHz, $CDCl_3$) δ 1.34 (s, 3H), 1.64 to 1.85 (m, 4H), 1.95 to 2.09 (m, 2H), 2.42 to 2.47 (m, 2H), 3.34 to 3.39 (m, 2H), 3.70 (s, 3H); ^{13}C NMR (75 MHz, $CDCl_3$) δ 21.9, 25.8, 27.8, 27.9, 30.6, 51.8, 52.8, 53.8, 78.5, 79.9, 172.9; IR (neat) 1737, 1438, 1294, 1197, 1118, 877 cm^{-1}; MS *m/z* (+EI) 228 (M^+, 4), 195 (+EI, 30), 137 (+EI, 27), 109 (+EI, 74), 43 (+EI, 100); HRMS (+EI) $(M+Na)^+$ found, 251.0892; $(M + Na)^+$ calculated for $C_{11}H_{16}O_5Na$, 251.0895.

(±)(1*R*,2*R*,4*S*,5*R*)Methyl 3-(5-methyl-3,6,7-trioxatricyclo[3.2.2.02,4]nonane)propanoate (compound 4d). Yield, 113 mg (43%); colorless oil; R_f, 0.13 (3:7 ethyl acetate-hexane); ^{1}H NMR (300 MHz, $CDCl_3$) δ 1.33 (s, 3H), 1.67 to 2.09 (m, 6H), 2.54 (t, J = 8.0 Hz, 2H), 3.27 (dd, J = 12.0, 5.0 Hz, 2H), 3.69 (s, 3H); ^{13}C NMR (75 MHz, $CDCl_3$) δ 21.5, 27.8, 27.9, 29.0, 31.1, 51.7, 52.1, 52.6, 74.0, 75.6, 173.4; IR (neat) 1737, 1438, 1303, 1197, 885, 725 cm^{-1}; MS *m/z* (+EI) 228 (M^+, 12), 196, (+EI, 56), 168 (+EI, 22), 115 (+EI, 44), 43 (+EI, 100); HRMS (+EI) $(M + Na)^+$ found, 251.0895; $(M + Na)^+$ calculated for $C_{11}H_{16}O_5Na$, 251.0895.

RESULTS

Chemistry. Building on our previous research into epoxy-endoperoxides as antimalarial drug candidates (64), we have examined the epoxides of bicyclic endoperoxides 2a to 2d, which contain tetrasubstituted carbons adjacent to the peroxide linkage. Endoperoxides 2a and 2c have previously been

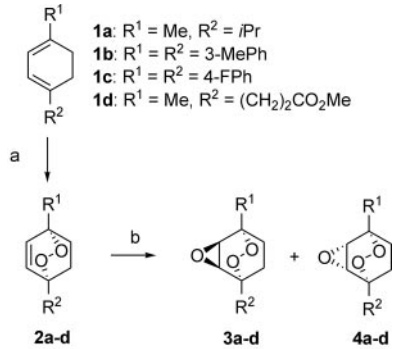

Scheme 1

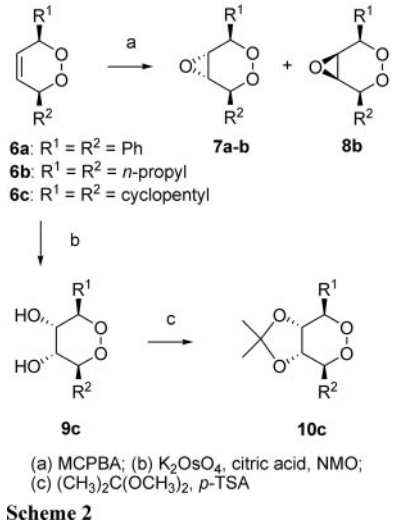

Scheme 2

FIG. 1. Schemes for the synthesis of endoperoxides. Me, methyl; *i*Pr, *iso*-propyl; MePh, methylphenyl; FPh, fluorophenyl; MCPBA, *meta*-chloroperbenzoic acid; *p*-TSA, *para*-toluenesulfonic acid; NMo, *N*-methylmorpholine-*N*-oxide.

assessed as antimalarials against the NF54 strain of *P. falciparum* (54). Epoxidation of these endoperoxides gave two isomers with the epoxide *trans* (compound 3) and *cis* (compound 4) to the peroxide linkage (Fig. 1, scheme 1). Ascaridole (compound 2a) was synthesized by photo-oxidation of α-terpinene (28) and was epoxidized as outlined by Turner and Herz (67). The stereochemistry of compounds 3a and 4a was then conclusively assigned through two-dimensional 2D ROESY (rotational nuclear Overhauser effect spectroscopy) NMR of the ring-opened derivative of compound 3a, confirming that it had the stereochemistry tentatively assigned by Turner and Herz (67). Endoperoxide 2b was synthesized as outlined by Posner et al. (54), with epoxidation performed as was done with the ascaridole derivatives (Fig. 1, scheme 1) and stereochemical determination through two-dimensional ROESY NMR of the epoxides. Synthesis of the 4-fluoro diene, compound 1c, was achieved through a route alternative to that used by Posner et al. (54).

Antimalarial activity. The abilities of the endoperoxides to inhibit the growth of CQ-sensitive strain D10 of *P. falciparum* during a 48-h in vitro culture period were determined (Table 1) and compared with data for CQ and artemisinin and previously generated monocyclic endoperoxides 6a, 6b, 7a, and 7b (64) and some novel derivatives, compounds 9c and 10c (62) (Fig. 1, scheme 2). The most active compounds were also tested against the CQ-resistant strain (strain K1) (Table 1). The compounds showed activity against the CQ-resistant strain similar to or higher than that against the CQ-sensitive strain. The activities of the bicyclic epoxy-endoperoxides and their parent endoperoxides were significantly better than those of similarly substituted monocyclic versions; compare the data for compounds 6a and 2b, 6b and 2a, 7a and 3b, or 7b and 3a.

Interaction of the novel endoperoxides with artemisinin. It was previously reported that the synthetic trioxolane endoperoxide (OZ277) interacts antagonistically with artemisinin against *P. falciparum* in vitro (69). We have examined the interactions between artemisinin and compounds 3a and 3c. The drugs were diluted over a 300-fold range starting with different fixed ratios of the test compounds (Table 2). The IC_{50} values for the inhibition of parasite growth (strain D10) were determined for each combination of drugs (Table 2), and the data were used to estimate the SFIC values (Table 2) and to prepare isobolograms (Fig. 2). A concave curve indicates a synergistic interaction, a convex curve indicates an antagonistic interaction, and a straight line indicates no interaction (7). Similarly, the SFIC value gives a numerical indication of an antagonistic interaction. An SFIC value of greater than 4 is indicative of strong antagonism. The slightly convex data set observed for the artemisinin combinations with compound 3a or 3c and SFIC values slightly greater than 1 indicate no interaction or an indeterminate interaction between these drugs.

Effect on parasite ultrastructure. In an attempt to obtain more information about the mechanisms of action of the novel endoperoxides, we examined the effects of artemisinin and the novel endoperoxides (compounds 3a and 3c) on the parasite ultrastructure. Trophozoite-stage parasite cultures (strain

TABLE 1. Biological activities of the novel endoperoxides

Compound	Antimalarial activity (IC_{50} [μM])	
	Strain D10	Strain K1
Artemisinin	0.013 ± 0.003	0.011
CQ	0.03 ± 0.01	0.66 ± 0.02
6a	6[a]	
7a	>10[a]	
6b	>10[a]	
7b	>10[a]	
2a	0.36 ± 0.04	0.15
3a	0.29 ± 0.06	0.12 ± 0.02
4a	0.80 ± 0.02	0.37
2b	0.79 ± 0.01	
3b	0.25 ± 0.04	0.39 ± 0.12
4b	1.96 ± 0.29	
2c	0.29 ± 0.06	0.23 ± 0.01
3c	0.1 ± 0.01	0.08 ± 0.02
4c	0.36 ± 0.06	0.16 ± 0.04
2d	5 ± 2.2	
3d	1.4 ± 0.46	
4d	7.2	
9c	6 + 0.9	
10c	7.2 ± 0.3	

[a] Data are from Taylor et al. (65).

TABLE 2. Interaction of two of the novel endoperoxides with artemisinin

Starting conc (μM) of artemisinin[a]	Assays with compound 3a				Assays with compound 3c			
	Starting conc (μM) of compound 3a[a]	Apparent IC_{50} (μM)		SFIC	Starting conc (μM) of compound 3c	IC_{50} (μM)		SFIC
		Artemisinin	Compound 3a			Artemisinin	Compound 3c	
0.04	0.09	0.0016	0.032	1.30 ± 0.48	0.035	0.038 Art	0.023	1.84 ± 0.43
0.02	0.18	0.0012	0.10	1.22 ± 0.18	0.075	0.048 μM Art	0.051	1.36 ± 0.11
0.01	0.35	0.0010	0.32	1.22 ± 0.14	0.15	0.08 μM Art	0.092	1.25 ± 0.13
0.005	0.70	0.0002	0.29	1.11 ± 0.03	0.30	0.15 μM Art	0.095	0.98 ± 0.03

[a] Twofold dilutions of the drugs combined in a fixed ratio were added to *P. falciparum* parasites (strain D10), and the incorporation of [^{3}H]hypoxanthine was determined over a 48-h incubation period. The apparent IC_{50} values for each of the drugs were estimated as though each drug had been added in isolation and were divided by the IC_{50} for the drug used alone to give the FICs. The individual FICs were used to calculate the SFICs. The results represent the means ± standard deviations of experiments performed in triplicate on three separate days. The IC_{50} values for the individual drugs determined for the artemisinin and compound 3a set were 0.011 ± 0.003 μM for artemisinin and 0.24 ± 0.05 μM for compound 3a, and for the IC_{50} values for the individual drugs determined for the artemisinin and compound 3c set were 0.015 ± 0.004 μM for artemisinin and 0.11 ± 0.02 μM for compound 3c.

D10) were treated for 4 or 8 h with 40 times the IC_{50} value (determined from the 48-h growth assay) and examined by transmission electron microscopy. Alternatively, ring-stage parasite cultures were treated for 24 h with approximately twice the IC_{50} value.

In control trophozoite-stage parasites (Fig. 3a and i; see Fig. S1 in the supplemental material), a dominant feature is the presence of hemozoin crystals contained within a clearly delineated digestive vacuole. Large vesicles containing hemoglobin taken up from the host cell cytoplasm (endocytic vesicles) are seen as more darkly staining structures. The parasite cytoplasm is heavily dotted with ribosomes and contains a clearly defined nucleus. Trophozoite-infected RBCs treated for 4 h with high concentrations of either artemisinin or compound 3a or 3c did not exhibit a major restructuring compared with the structure of the control cells; however, there was a loss of digestive vacuole integrity in some artemisinin-treated cells (see Fig. S1b in the supplemental material) and a buildup of endocytic vesicles in some compound 3a- and compound 3c-treated cells (see Fig. S1c and d in the supplemental material). After 8 h of treatment with the endoperoxide antimalarials, more dramatic effects on parasite morphology were observed. In many of the artemisinin-treated parasites, the digestive vacuole membrane was disrupted and the hemozoin crystals were in contact with the parasite cytoplasm (Fig. 3b; see Fig. S1f in the supplemental material). By contrast, trophozoites treated with the novel endoperoxides showed an accumulation of undigested hemoglobin-containing endocytic vesicles, many of which appeared to be located within the digestive vacuole membrane (Fig. 3c and d; see Fig. S1g and h in the supplemental material). After the 8-h incubation period, some cells had reached the schizont stage (Fig. 3e to h). Control schizonts showed the developing merozoites with clearly defined nuclei, darkly staining rhoptries, and dense granules (Fig. 3e). Artemisinin-treated schizonts again showed a loss of the digestive vacuole membrane and aberrant merozoite morphology (Fig. 3f). Schizonts incubated with compounds 3a and 3c showed highly misshapen merozoites with uneven staining of the nucleus (Fig. 3g and h) and an accumulation of darkly stained vesicular structures (Fig. 3g, asterisk).

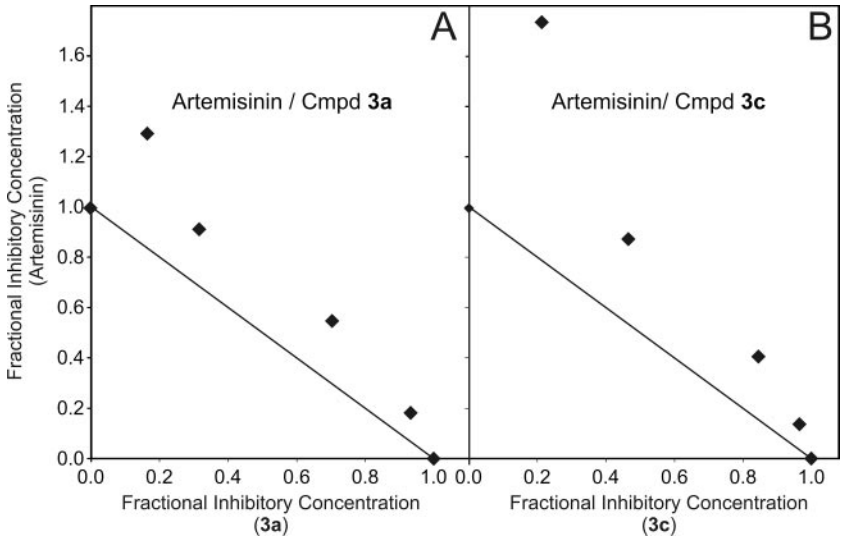

FIG. 2. Interaction of artemisinin and two novel endoperoxides in inhibiting parasite growth. Isobolograms were constructed from the IC_{50} values in Table 2. For each drug combination, FICs were calculated by dividing the measured apparent IC_{50} values for the individual drugs in the different combinations of artemisinin with compound (Cmpd) 3a (A) or compound 3c (B) by the IC_{50} values obtained when the drugs were used alone.

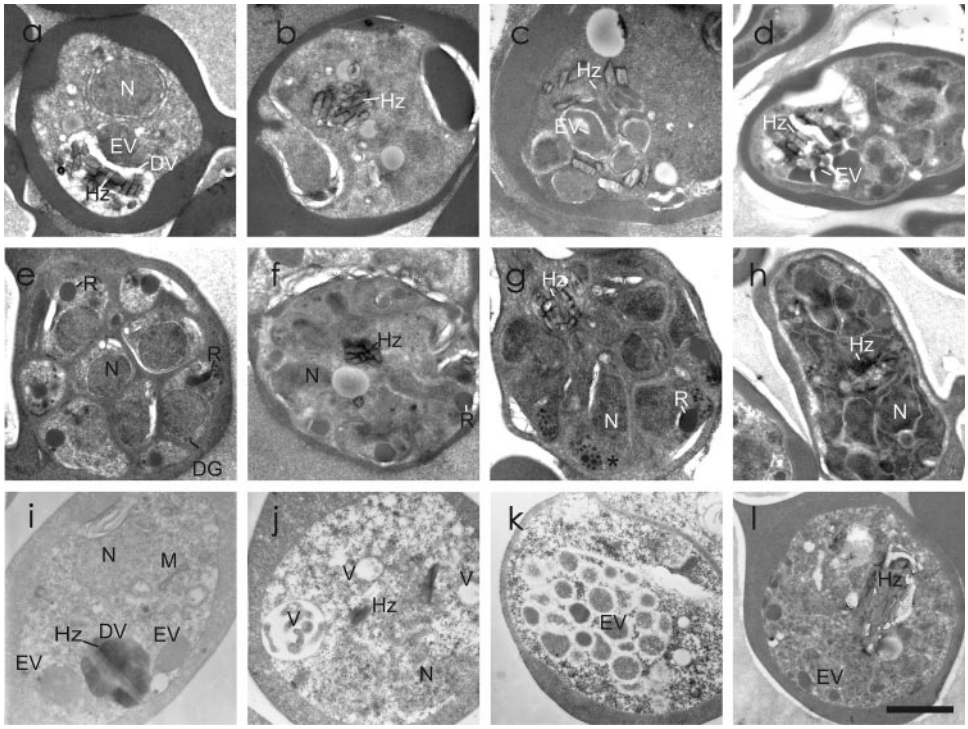

FIG. 3. Transmission electron microscopy analysis of endoperoxide-treated parasitized RBCs. Trophozoite-stage parasite-infected RBCs (strain D10) were incubated with no drug (a and e) or 40 times the IC_{50} values of artemisinin (b and f), compound 3a (c and g), or compound 3c (d and h) for 8 h. Alternatively, ring-stage parasite-infected RBCs were incubated with no drug (i) or two times the IC_{50} values of artemisinin (j), compound 3a (k), or compound 3c (l) for 24 h. Sections through the control trophozoite-stage parasites (a and i) show endocytic vesicles (EV) and typical hemozoin crystals (Hz) within a digestive vacuole (DV). The parasite cytoplasm is dotted with ribosomes and has a defined nucleus (N). The mitochondrion (M) is visible in some sections (i). Schizonts (e) show well-defined nuclei and developing apical organelles, rhoptries (R), and dense granules (DG). After an 8-h treatment with a high concentration of artemisinin, both trophozoite-stage parasites (b) and schizont-stage parasites (j) show the loss of digestive vacuole integrity. Many of the infected RBCs treated for 24 h with artemisinin (j) show a substantial loss of membranous features, with individual hemozoin crystals in contact with the parasite cytoplasm and the formation of vacuoles (V). Trophozoites treated for 8 h with 40 times the IC_{50} value of compound 3a (c) or compound 3c (d) show an accumulation of undigested endocytic vesicles in the digestive vacuole. Schizonts in the samples treated for 8 h with compound 3a (g) or compound 3c (h) show merozoites with an aberrant morphology and uneven staining of the nucleus. There is an accumulation of dense vesicles (g, asterisk) in many cells. Infected RBCs treated for 24 h with two times the IC_{50} value of compound 3a show an accumulation of endocytic vesicles (EV) and myelin bodies (MB) (see Fig. S1k in the supplemental material). Compound 3c causes less obvious damage (l), but development seems to be inhibited and very few schizonts are observed. Bar, 1 μm. Additional images are presented in Fig. S1 in the supplemental material.

Ring-stage parasite-infected RBCs treated for 24 h with artemisinin at two times its IC_{50} value (Fig. 3j; see Fig. S1j in the supplemental material) advanced to the trophozoite stage but showed a marked loss of organellar structures accompanied by the disintegration of many of the major membrane-bound features. In particular, the loss of the digestive vacuole membrane often left individual hemozoin crystals in direct contact with the parasite cytoplasm. Vacuoles were observed in some cells (Fig. 3j). Infected RBCs treated for 24 h with twice the IC_{50} value of compound 3a or 3c (Fig. 3k and l) showed a less obvious loss of membrane structures; however, a major feature was the appearance of large vacuoles and myelin bodies as well as hemoglobin-containing endocytic vesicles (Fig. 3k and l; see Fig. S1k and l in the supplemental material). Similar effects of the different drug treatments on parasite morphology were observed with strain 3D7 parasites.

Effect of endoperoxides on digestive vacuole integrity. Because of the difficulty of quantitating the effects of the compounds on the ultrastructural morphology, we have developed a series of fluorescence microscopy-based techniques to assess damage to different organelles within infected RBCs. In an effort to visualize damage to the digestive vacuole we have made use of the pH-sensitive probe LysoSensor Blue. This probe is a weak base that accumulates in acidic compartments (38, 72). In mid-trophozoite-stage parasites, the probe is concentrated in the digestive vacuole (as judged by the overlap with the hemozoin location); however, there is also some weak labeling of the parasite cytoplasm (Fig. 4A, panels a and e). The fluorescence profile was independent of the time of incubation with LysoSensor Blue, indicating that the weak base probe does not induce a change in the pH of the labeled compartment. The LysoSensor Blue fluorescence also colocalizes with the fluorescence of plasmepsin-green fluorescent protein (31) in transfected parasites expressing this digestive vacuole-located chimeric protein (data not shown).

The infected RBCs were treated with artemisinin, compound 3a, or compound 3c for 4 or 8 h at different concentrations. Even after only 4 h of treatment with artemisinin, a substantial proportion of the parasite population showed alterations in LysoSensor Blue labeling. The probe was redis-

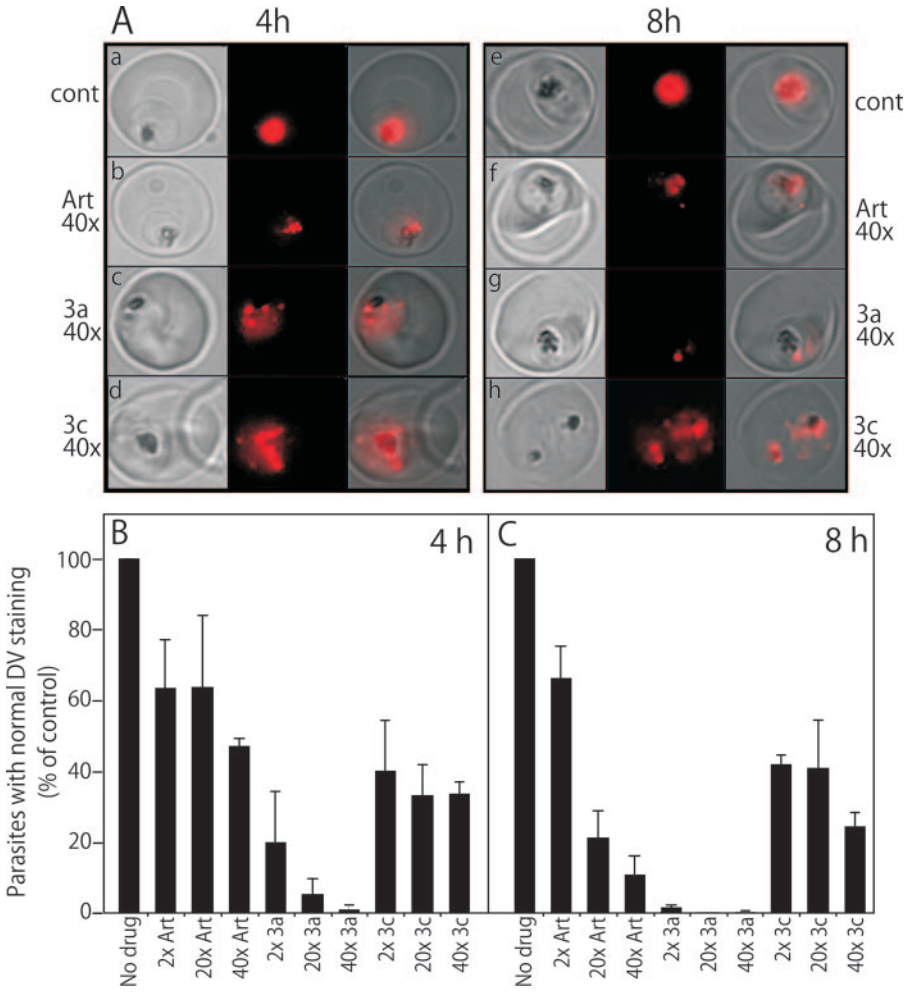

FIG. 4. Analysis of digestive vacuole integrity in endoperoxide-treated parasitized RBCs. Strain D10 parasites at the trophozoite stage were incubated with no additions or 2, 20, or 40 times the IC_{50} values of artemisinin, compound 3a, or compound 3a for 4 or 8 h. LysoSensor Blue was used to probe acidic compartments, with imaging performed by fluorescence microscopy. (A) Bright-field, fluorescence signals and overlays of control and drug-treated parasites. (B and C) The LysoSensor Blue labeling pattern in infected RBCs (300 cells) in cultures that were drug treated for 4 (B) or 8 h (C) was classified as normal or redistributed. Data are normalized relative to those for the control, to which no drug was added, and represent the means ± standard deviations of data from three separate experiments. cont, control; DV, digestive vacuole; Art, artemisinin.

tributed to punctate structures either associated with the digestive vacuole or in the parasite cytoplasm (Fig. 4A, panel b). After 8 h at 20 to 40 times the IC_{50} value of artemisinin, most of the cells in the population showed an altered distribution of the fluorescent probe (Fig. 4A, panel f), and many parasites showed a complete loss of the fluorescence signal (data not shown). The novel endoperoxides, at 20 to 40 times their respective IC_{50} values, also caused substantial changes to the distribution of the LysoSensor Blue probe (Fig. 4A, panels c, d, g, and h), with the LysoSensor Blue-stained compartments often appearing fragmented or dispersed. This suggests that compounds 3a and 3c also disrupt the function of the digestive vacuole. The redistribution and loss of LysoSensor Blue may indicate a restructuring of this compartment and the loss of the digestive vacuole pH gradient, respectively. The punctate structures that accumulate the pH probe in compound 3a- and 3c-treated parasites may represent the accumulated endocytic vesicles observed by electron microscopy.

We have made a semiquantitative analysis of the effects of the different compounds on LysoSensor Blue staining (Fig. 4B and C). After 8 h of treatment with 20 to 40 times the IC_{50} value of artemisinin, more than 80% of the parasites showed altered digestive vacuole staining. Similar effects were observed with the novel endoperoxides. Treatment with compound 3a for 8 h at only two times its IC_{50} value resulted in an altered distribution of the pH sensor in more than 80% of the parasites (Fig. 4C), with a complete loss of the fluorescence signal in many parasites (data not shown). The data further indicate that disruption of the integrity of the digestive vacuole may be an early event in the mechanism of action of endoperoxide antimalarials.

Effect of endoperoxides on ER morphology and interactions with ER Ca^{2+} ATPase inhibitors. Recently, it was shown that artemisinin inhibits the activity of the ER protein SERCA (also known as PfATPase6) in an oocyte expression model (68), and it was proposed that SERCA is a major downstream target of artemisinin (15, 68). We have examined the abilities of thapsigargin (a sesquiterpene lactone that is a specific

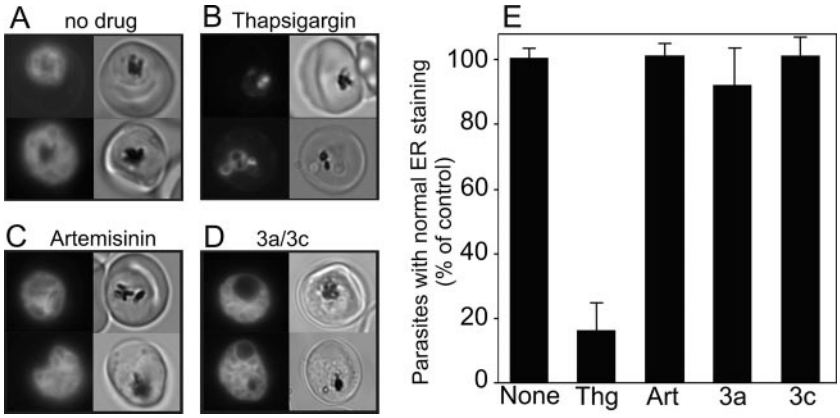

FIG. 5. Analysis of morphology of the ER in endoperoxide-treated parasitized RBCs. Strain D10 parasites at the trophozoite stage were incubated with (A) no additions or 10 times the IC_{50} values of (B) thapsigargin, (C) artemisinin, (D, upper panel) compound 3a, or (D, lower panel) compound 3c for 12 h. ER Tracker was used to label the ER before imaging by fluorescence microscopy. (B) Fluorescence images of infected RBCs (300 cells) were classified as normal or condensed. Data are normalized relative to those for the control, to which no drug was added, and represent the means ± standard deviations of data from three separate experiments.

SERCA inhibitor) and the endoperoxides to alter the morphology of the ER as defined by the ER-selective probe ER Tracker Blue-White. The ER appears as a reticular network in the cytoplasm of the parasite (Fig. 5A). After a 12-h treatment of trophozoite-stage parasites with 10 times the IC_{50} value of thapsigargin, a marked contraction and reorganization of the ER was observed (Fig. 5B). By contrast, artemisinin, compound 3a, and compound 3c at 10 times their respective IC_{50} values had no major effect on the morphology of the ER (Fig. 5C and D). We made a semiquantitative analysis of the effects of the different compounds (Fig. 5E). The effect of thapsigargin on the morphology of the ER was much more marked than that of the endoperoxides. This suggests that the endoperoxides may exert their activities by a mode of action different from that of thapsigargin.

It was previously reported that thapsigargin antagonizes the plasmocidal activity of artemisinin (68). We examined the interactions between thapsigargin and artemisinin and between thapsigargin and compounds 3a and 3c. We found that thapsigargin inhibited the parasite growth of strains D10 and 3D7 of *P. falciparum*, with IC_{50} values of 7.2 ± 1.6 μM and 4.2 ± 0.5 μM, respectively. These values are slightly higher than the value previously reported for strain 3D7 (68). We undertook an analysis of the interactions of these compounds (against strain D10) to estimate the SFIC values (Table 3) and to prepare isobolograms (Fig. 6). The slightly concave data set observed for the thapsigargin-artemisinin combination and SFIC values slightly less than 1 do not support the previously reported antagonism between these drugs. Similar results were obtained for a combination of artemisinin and thapsigargin against strain 3D7 (data not shown). Similarly, we found no evidence for an interaction between compounds 3a and 3c and thapsigargin in strain D10 (Table 3; Fig. 6B and C). The same result was obtained for compounds 3a and 3c with thapsigargin in strain 3D7 (data not shown).

Effects of endoperoxides on mitochondrial morphology and membrane potential. Components of the mitochondrial electron transport chain in yeast have been shown to be susceptible to artemisinin (36). To further examine the mode of action of artemisinin and the novel endoperoxides, we have used rhodamine 123, a membrane potential-dependent probe, to detect mitochondrial damage. In control infected RBCs, rhodamine 123 accumulated within the slender branched mitochondrion of *P. falciparum* (Fig. 7A), as reported previously (14). Treatment of infected RBCs with monesin and nigericin dissipates the membrane potential and completely abrogates the fluorescence signal (Fig. 7B). By contrast, the treatment of infected RBCs for 4 h with 40 times the IC_{50} values of artemisinin and compound 3a had no obvious effect on the morphology of the mitochondrion (Fig. 7C and D). To obtain a more quantitative

TABLE 3. Interaction of artemisinin and two novel endoperoxides with thapsigargin

Starting concn (μM) of thapsigargin[a]	Assays with artemisinin				Assays with compound 3a				Assays with compound 3c			
	Artemisinin concn (μM)	Apparent IC_{50} (μM)		SFIC	Starting concn (μM) of compound 3a	Apparent IC_{50} (μM)		SFIC	Starting concn (μM) of compound 3c	Apparent IC_{50} (μM)		SFIC
		Artemisinin	Thapsigargin			Compound 3a	Thapsigargin			Compound 3c	Thapsigargin	
2.5	0.04	0.010	0.31	1.04	1.6	0.14	0.22	0.8	0.6	0.10	0.42	0.97
5.0	0.02	0.0072	0.83	0.83	0.8	0.14	0.93	0.8	0.3	0.068	1.12	0.77
10.0	0.01	0.0054	2.33	0.85	0.4	0.079	2.0	0.71	0.15	0.048	3.02	0.84

[a] Twofold dilutions of the drugs combined in a fixed ratio were added to *P. falciparum* parasites (strain D10). The apparent IC_{50} values for each of the drugs were estimated and used to calculate the SFIC values. The results represent the mean values for an experiment performed in duplicate. The IC_{50} values for the individual drugs determined for this data set were 7.4 μM for thapsigargin, 0.010 μM for artemisinin, 0.18 μM for compound 3a, and 0.11 μM for compound 3c.

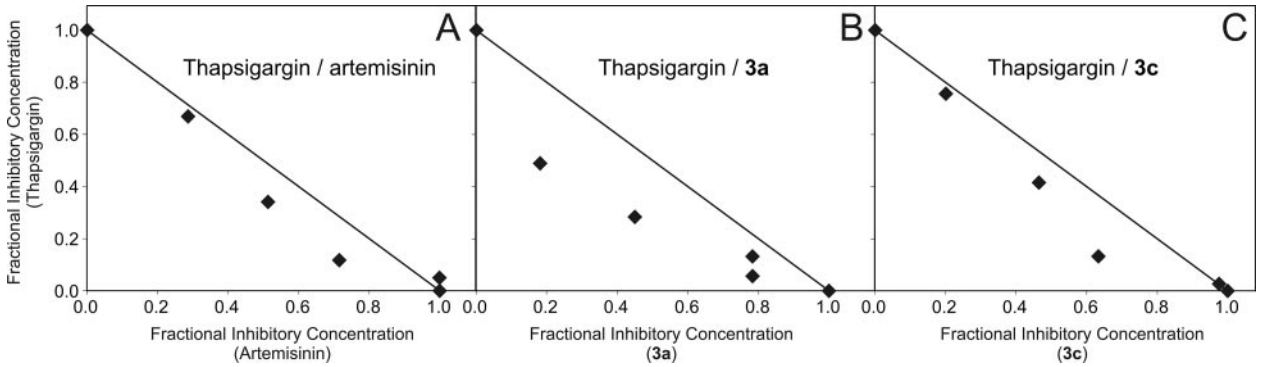

FIG. 6. Interaction of endoperoxide and thapsigarin in parasite killing. Isobolograms were constructed from the IC_{50} values in Table 3. For each drug combination, the FICs were calculated by dividing the measured apparent IC_{50} values for individual drugs in the different combinations of thapsigargin with artemisinin (A), compound 3a (B), or compound 3c (C) by the IC_{50} values obtained when the drugs were used alone.

analysis of the effects of the endoperoxides, artemisinin and compound 3a were added at concentrations corresponding to 2, 20, and 40 times their IC_{50} values to parasites in the ring or trophozoite stage, and the ring- and trophozoite-stage parasites were then returned to culture for 24 and 4 h, respectively, before they were stained with rhodamine 123. Trophozoite-stage parasites treated for 4 h with the drugs showed relatively little effect on mitochondrial potential even at the highest drug

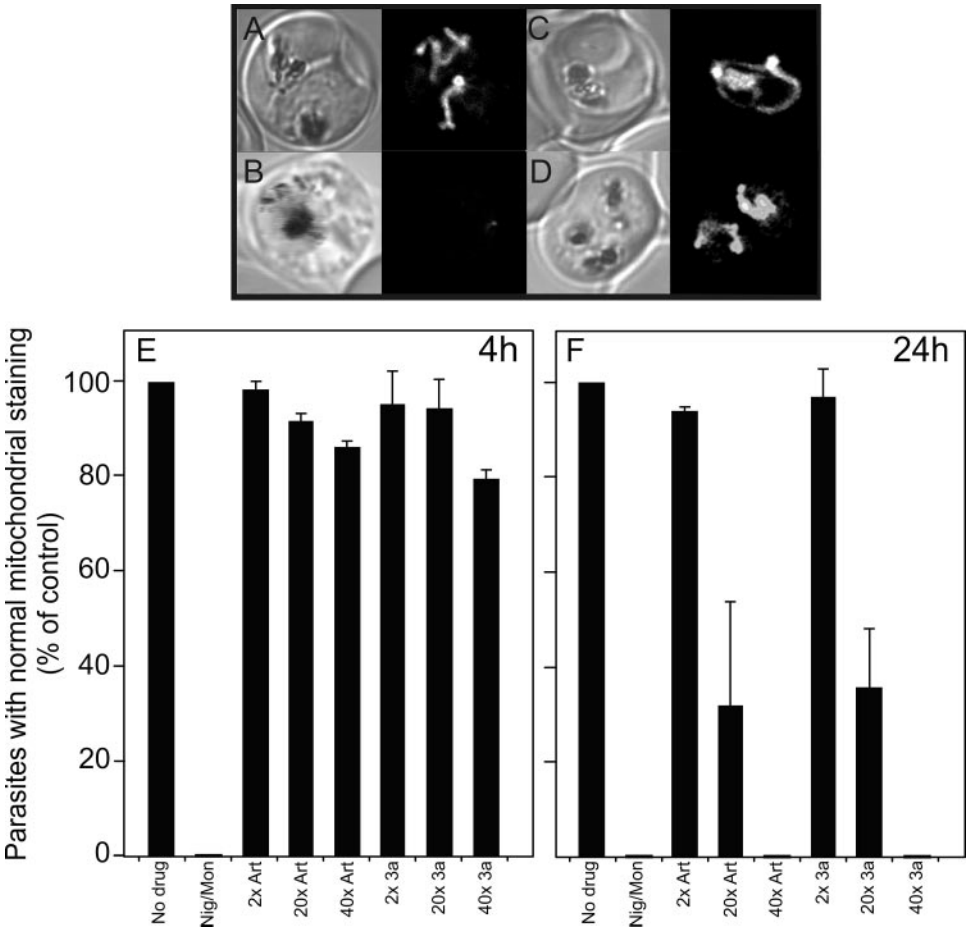

FIG. 7. Analysis of mitochondrial function in endoperoxide-treated parasitized RBCs. Strain D10 trophozoite-stage parasite-infected RBCs were incubated with (A) no additions, (B) the ionophores nigericin and monensin (20 μM each), or 40 times the IC_{50} values of (C) artemisinin or (D) compound 3a for 4 h. Rhodamine 123 (0.2 μM) was used to stain the mitochondrion for confocal microscopy. (E) Trophozoite-stage parasites were incubated for 4 h or (F) ring-stage infected RBCs were incubated for 24 h with no drug or with 2, 20, or 40 times the IC_{50} values of artemisinin or compound 3a. Infected RBCs (1,000 cells) were counted and classified as normal or rhodamine 123 depleted by fluorescence microscopy. Data are normalized relative to those for the control, to which no drug was added.

concentrations examined (Fig. 7E), indicating that the loss of mitochondrial function is not an early event in the action of either artemisinin or compound 3a. After treatment of the ring-stage parasites for 24 h with artemisinin or compound 3a at twice the IC_{50} value, the mitochondrial membrane potential appeared to be at least partially intact (Fig. 7F), despite the significant disruption to the membrane structures observed by electron microscopy. This suggests that disruption of the mitochondrion is probably not the mode of action of either drug. Higher concentrations of the drug did impair rhodamine 123 accumulation (Fig. 7F), but this is probably consequent upon rather than responsible for parasite killing.

DISCUSSION

We have generated a novel series of bicyclic endoperoxides that inhibit parasite growth at IC_{50} values down to 80 nM. This is a significant improvement compared with the findings for our previously synthesized monocyclic compounds, compounds 6a, 6b 7a, and 7b (Table 1), and supports our suggestion that tetrasubstitution of the carbons adjacent to the peroxide linkage is important for antimalarial activity. The most active compounds (compounds 3a to 3c; 0.08 to 0.29 μM) were less potent than artemisinin (~10 nM) and were also about threefold less active than CQ against the CQ-sensitive strain (0.03 μM); however, they were much more active than CQ against CQ-resistant strains (IC_{50} value, 0.66 μM; Table 1) and their activity was similar to or better than that of sulfadoxine (~0.1 μM for sensitive strains and up to 10 μM for resistant strains) (57). Two of the parent endoperoxide compounds (compounds 2a and 2c) have previously been tested for their antimalarial activities against a CQ-sensitive strain (54). The IC_{50} value reported here for compound 2c (0.23 to 0.29 μM) is somewhat higher than the value (0.07 μM) reported previously. This may reflect the shorter growth inhibition time and different strain of *P. falciparum* used in our assay, as our IC_{50} value for CQ against D10 was also higher (0.03 μM) than the value obtained by Posner et al. (0.005 μM) (54). The IC_{50} value reported here for compound 2a (0.36 μM) is somewhat lower than the value (0.65 μM) reported previously, but the authors noted that this compound was volatile and that its activity may have been underestimated (54).

Interestingly, the *trans* isomers of the bicyclic endoperoxides were more active than the *cis* isomers. By contrast, we previously found that *cis*-epoxides of the monocyclic endoperoxides were more active than their *trans* counterparts (64). This suggests that the spatial placement of the epoxide oxygen is important for binding to a putative endoperoxide target but that the optimal position depends on other substituents on the endoperoxide ring system. The endoperoxide parents of the bicyclic epoxy-endoperoxides showed significantly lower levels of activity than the *trans*-epoxides but levels of activity similar to or even better than those of the *cis*-epoxides. This suggests that it is the position of the endoperoxide oxygen rather than its electron-withdrawing effects that determines its increased activity. Dihydroxy compound 9c and its acetonide derivative, compound 10c (64), showed much lower levels of activity, indicating that an epoxy substituent is more effective at promoting activation of the endoperoxide. Similarly, the inclusion of an ester group on the alkyl side chain significantly decreased the level of activity (compounds 2 to 4d).

The main advantage of our novel class of compounds is their ease of synthesis (and, thus, low cost). We have shown that the *trans*-epoxide derivatives exhibit maximum activity, indicating that the position of the epoxide oxygen plays an important role in determining the activity of the endoperoxide. This is in keeping with the suggestion that the activated endoperoxides exert their lethal effects by binding to and damaging particular proteins rather than by causing more general damage as rapidly diffusing free radical species. These epoxy-endoperoxides are readily synthesized and represent good lead compounds for the development of highly effective and inexpensive endoperoxide antimalarials; however, further development of these compounds will require the demonstration of their activity in vivo.

The compounds provide us with a useful tool with which the mechanism(s) of action of endoperoxide antimalarials can be studied. The precise mode of action of artemisinin and its derivatives is still a matter of some debate; however, it has been shown that [^{14}C]artemisinin accumulates in the digestive vacuole and mitochondria and that artemisinin treatment induces morphological changes to the mitochondria, rough ER, nuclear envelope, and digestive vacuole (39, 44).

To investigate the likely mode of action of the novel endoperoxides, we have examined their effects on the cellular ultrastructure. Given that activated endoperoxide antimalarials are thought to exert their activity by alkylating specific protein or lipid targets, we reasoned that this is likely to cause early morphological alterations to the organelle in which the target is located. Indeed, when trophozoite-infected RBCs were treated for 4 to 8 h with high concentrations of artemisinin, we observed a loss of digestive vacuole integrity in many cells. This suggests that artemisinin exerts its activity by alkylating the protein and lipid components of the digestive vacuole membrane. This suggestion is supported by the findings of a number of previous studies (8, 9, 39, 50, 61). A longer incubation of infected RBCs with two times the IC_{50} value of artemisinin caused a marked disintegration of many of the major membrane-bound features. This general loss of membrane structure in artemisinin-treated cells has also been noted previously (29, 30, 39).

Interestingly, trophozoites treated for 4 to 8 h with high concentrations of compound 3a or 3c did not show a loss of digestive vacuole integrity but did exhibit a buildup of undigested endocytic vesicles within the digestive vacuole. Schizont-stage parasites also showed abnormal nuclear staining and morphology. A buildup of hemoglobin-containing vesicles in the parasite cytoplasm or in the digestive vacuole has been observed previously upon the treatment of infected RBCs with quinolines (16, 25, 73), and hemoglobin accumulation in the digestive vacuole is observed upon treatment with protease inhibitors (63). The buildup of intact endocytic vesicles within the confines of the digestive vacuole suggests that the endoperoxides may inhibit the phospholipases that are needed to degrade the membranes of endocytic vesicles (32, 33). In contrast to artemisinin, longer periods of incubation with lower concentrations of the novel endoperoxides did not cause an extensive loss of membranous features, indicating that they kill parasites without complete disruption of the cells. A major

ultrastructural feature was the accumulation of endocytic vesicles, vacuoles. and myelin bodies. Multilamellar structures have also been reported previously following the treatment of parasites with quinoline antimalarials (46). Thus, the data indicate that both artemisinin and the novel endoperoxides have an early effect on digestive vacuole function; however, this effect may have a different molecular basis.

We also used a fluorescent pH probe to monitor the integrity of the digestive vacuole. We observed substantial alterations in the distribution of the probe after only a few hours of treatment with physiologically relevant concentrations of artemisinin or the novel endoperoxides. While it remains possible that the reorganization of the digestive vacuole is a downstream consequence of damage to a protein in another compartment, our work supports the findings of previous studies implicating the digestive vacuole as a possible site of action of artemisinin (8, 9, 39, 50, 61).

By contrast, we found no early-stage effects of artemisinin or the novel endoperoxides on the morphology of the mitochondrion or the ER. Therefore, our data argue against the mitochondrion or the ER as the site of action of endoperoxides. Moreover, we also found no interaction of the endoperoxides with thapsigargin, which argues against the suggestion that the endoperoxides exert their activity by inhibiting the activity of SERCA. It is not clear why we failed to observe the previously reported antagonism. Our experiments were performed on several different days with two different strains of the parasite; however, it remains possible that differences in experimental design led to different observed interactions. In this context it is interesting to note that the synthetic endoperoxide OZ277 was recently shown to be only a weak inhibitor of SERCA activity (69). Moreover, a genetic analysis (2) showed no mutations in SERCA in artemisinin-resistant *P. chabaudi* and *P. falciparum*. We conclude that the previously reported antagonistic interactions between artemisinin and thapsigargin under some experimental conditions may not reflect a real intersection of biochemical pathways.

It is interesting to speculate on the mechanism by which artemisinin might induce early damage to the digestive vacuole membrane. It is possible that some of the heme that is released during hemoglobin digestion escapes conversion to hemozoin and accumulates in the digestive vacuole membrane. Artemisinin may interact with (and be activated by) this membrane-bound heme and cause early damage to the integrity of the digestive vacuole membrane. By contrast, the novel endoperoxides may preferentially target digestive vacuole enzymes, including phospholipases, leading to the inhibition of hemoglobin digestion.

Our findings suggest that the mode of action of endoperoxide antimalarials needs to be reevaluated and that digestive vacuole targets should be further examined. We suggest that the LysoSensor Blue-based assay could be used for the rapid screening of much needed new endoperoxide antimalarials.

ACKNOWLEDGMENTS

This work was supported by the National Health and Medical Research Council and the Australian Research Council.

We thank Sam Deed for technical support; Nick Klonis for technical advice; and Mike Klemba, Virginia State University, for supplying the plasmepsin-green fluorescent protein transfectants.

REFERENCES

1. **Adovelande, J., J. Deleze, and J. Schrevel.** 1998. Synergy between two calcium channel blockers, verapamil and fantofarone (SR33557), in reversing chloroquine resistance in *Plasmodium falciparum*. Biochem. Pharmacol. **55:** 433–440.
2. **Afonso, A., P. Hunt, S. Cheesman, A. C. Alves, C. V. Cunha, V. do Rosario, and P. Cravo.** 2006. Malaria parasites can develop stable resistance to artemisinin but lack mutations in candidate genes *atp6* (encoding the sarcoplasmic and endoplasmic reticulum Ca^{2+} ATPase), *tctp*, *mdr1*, and *cg10*. Antimicrob. Agents Chemother. **50:**480–489.
3. **Aley, S. B., J. A. Sherwood, K. Marsh, O. Eidelman, and R. J. Howard.** 1986. Identification of isolate-specific proteins on sorbitol-enriched *Plasmodium falciparum* infected erythrocytes from Gambian patients. Parasitology **92:** 511–525.
4. **Arrow, K. J., C. B. Panosian, and H. Gelbrand.** 2004. Saving lives, buying time: economics of malaria drugs in an age of resistance. The National Academies Press, Washington, DC.
5. **Avery, M. A., W. K. M. Chong, and C. Jenning-White.** 1992. Stereroselective total synthesis of (+)-artemisinin, the antimalarial constituent of *Artemisia annua* L. J. Am. Chem. Soc. **114:**974–979.
6. **Avery, T. D., N. F. Jenkins, M. C. Kimber, D. W. Lupton, and D. K. Taylor.** 2002. First examples of the catalytic asymmetric ring-opening of meso-1,2-dioxines utilising cobalt(II) complexes with optically active tetradentate Schiff base ligands: formation of enantio-enriched cyclopropanes. Chem. Commun. (Cambridge), Issue 1, p.28–29.
7. **Berenbaum, M. C.** 1978. A method for testing for synergy with any number of agents. J. Infect. Dis. **137:**122–130.
8. **Berman, P. A., and P. A. Adams.** 1997. Artemisinin enhances heme-catalysed oxidation of lipid membranes. Free Radic. Biol. Med. **22:**1283–1288.
9. **Bhisutthibhan, J., X. Q. Pan, P. A. Hossler, D. J. Walker, C. A. Yowell, J. Carlton, J. B. Dame, and S. R. Meshnick.** 1998. The *Plasmodium falciparum* translationally controlled tumor protein homolog and its reaction with the antimalarial drug artemisinin. J. Biol. Chem. **273:**16192–16198.
10. **Borstnik, K., I. H. Paik, and G. H. Posner.** 2002. Malaria: new chemotherapeutic peroxide drugs. Mini Rev. Med. Chem. **2:**573–583.
11. **Borstnik, K., I. H. Paik, T. A. Shapiro, and G. H. Posner.** 2002. Antimalarial chemotherapeutic peroxides: artemisinin, yingzhaosu A and related compounds. Int. J. Parasitol. **32:**1661–1667.
12. **Bray, P. G., S. Deed, E. Fox, M. Kalkanidis, M. Mungthin, L. W. Deady, and L. Tilley.** 2005. Primaquine synergises the activity of chloroquine against chloroquine-resistant *P. falciparum*. Biochem. Pharmacol. **70:**1158–1166.
13. **Cheung, F. K., A. M. Hayes, J. Hannedouche, A. S. Yim, and M. Wills.** 2005. "Tethered" Ru(II) catalysts for asymmetric transfer hydrogenation of ketones. J. Org. Chem. **70:**3188–3197.
14. **Divo, A. A., T. Geary, J. Jensen, and H. Ginsburg.** 1985. The mitochondrion of Plasmodium falciparum visualized by rhodamine 123 fluorescence. J. Protozool. **32:**442–446.
15. **Eckstein-Ludwig, U., R. J. Webb, I. D. Van Goethem, J. M. East, A. G. Lee, M. Kimura, P. M. O'Neill, P. G. Bray, S. A. Ward, and S. Krishna.** 2003. Artemisinins target the SERCA of *Plasmodium falciparum*. Nature **424:**957–961.
16. **Fitch, C. D., G. Z. Cai, Y. F. Chen, and J. S. Ryerse.** 2003. Relationship of chloroquine-induced redistribution of a neutral aminopeptidase to hemoglobin accumulation in malaria parasites. Arch. Biochem. Biophys. **410:** 296–306.
17. **Foote, S. J., J. K. Thompson, A. F. Cowman, and D. J. Kemp.** 1989. Amplification of the multidrug resistance gene in some chloroquine-resistant isolates of *P. falciparum*. Cell **57:**921–930.
18. **Frankland, S., A. Adisa, P. Horrocks, T. F. Taraschi, T. Schneider, S. R. Elliott, S. J. Rogerson, E. Knuepfer, A. F. Cowman, C. I. Newbold, and L. Tilley.** 2006. Delivery of the malaria virulence protein PfEMP1 to the erythrocyte surface requires cholesterol-rich domains. Eukaryot. Cell **5:**849–860.
19. **Gardner, M. J., N. Hall, E. Fung, O. White, M. Berriman, R. W. Hyman, J. M. Carlton, A. Pain, K. E. Nelson, S. Bowman, I. T. Paulsen, K. James, J. A. Eisen, K. Rutherford, S. L. Salzberg, A. Craig, S. Kyes, M. S. Chan, V. Nene, S. J. Shallom, B. Suh, J. Peterson, S. Angiuoli, M. Pertea, J. Allen, J. Selengut, D. Haft, M. W. Mather, A. B. Vaidya, D. M. Martin, A. H. Fairlamb, M. J. Fraunholz, D. S. Roos, S. A. Ralph, G. I. McFadden, L. M. Cummings, G. M. Subramanian, C. Mungall, J. C. Venter, D. J. Carucci, S. L. Hoffman, C. Newbold, R. W. Davis, C. M. Fraser, and B. Barrell.** 2002. Genome sequence of the human malaria parasite *Plasmodium falciparum*. Nature **419:**498–511.
20. **Garner, P., and P. M. Graves.** 2005. The benefits of artemisinin combination therapy for malaria extend beyond the individual patient. PLoS Med. **2:**e105.
21. **Greatrex, B. W., N. F. Jenkins, D. K. Taylor, and E. R. Tiekink.** 2003. Base- and Co(II)-catalyzed ring-opening reactions of perhydrooxireno[2,3-d][1,2]dioxines: an efficient route to 4-hydroxy-2,3-epoxy-ketones. J. Org. Chem. **68:**5205–5210.
22. **Greatrex, B. W., and D. K. Taylor.** 2005. Ring-opening of unsymmetrical 1,2-dioxines using cobalt(II) salen complexes. J. Org. Chem. **70:**470–476.

23. **Haynes, R. K., and S. Krishna.** 2004. Artemisinins: activities and actions. Microbes Infect. **6:**1339–1346.
24. **Hindley, S., S. A. Ward, R. C. Storr, N. L. Searle, P. G. Bray, B. K. Park, J. Davies, and P. M. O'Neill.** 2002. Mechanism-based design of parasite-targeted artemisinin derivatives: synthesis and antimalarial activity of new diamine containing analogues. J. Med. Chem. **45:**1052–1063.
25. **Hoppe, H. C., D. A. van Schalkwyk, U. I. Wiehart, S. A. Meredith, J. Egan, and B. W. Weber.** 2004. Antimalarial quinolines and artemisinin inhibit endocytosis in *Plasmodium falciparum*. Antimicrob. Agents Chemother. **48:** 2370–2378.
26. **Jefford, C. W.** 2007. New developments in synthetic peroxidic drugs as artemisinin mimics. Drug Discov. Today **12:**487–495.
27. **Jefford, C. W.** 2001. Why artemisinin and certain synthetic peroxides are potent antimalarials. Implications for the mode of action. Curr. Med. Chem. **8:**1803–1826.
28. **Jefford, C. W., A. Jaber, and J. Boukouvalas.** 1989. The regio- and stereocontrolled synthesis of *cis-p*-menth-3-ene-1,2-diol by means of a 1,2,4-trioxane intermediate. Chem. Commun. **24:**1916–1918.
29. **Jiang, J. B., G. Jacobs, D. S. Liang, and M. Aikawa.** 1985. Quinghaosu-induced changes in the morphology of *Plasmodium inui*. Am. J. Trop. Med. Hyg. **34:**424–428.
30. **Kawai, S., S. Kano, and M. Suzuki.** 1993. Morphologic effects of artemether on *Plasmodium falciparum* in *Aotus trivigartus* Am. J. Trop. Med. Hyg. **49:**812–818.
31. **Klemba, M., W. Beatty, I. Gluzman, and D. E. Goldberg.** 2004. Trafficking of plasmepsin II to the food vacuole of the malaria parasite *Plasmodium falciparum*. J. Cell Biol. **164:**47–56.
32. **Krugliak, M., Z. Waldman, and H. Ginsburg.** 1987. Gentamicin and amikacin repress the growth of *Plasmodium falciparum* in culture, probably by inhibiting a parasite acid phospholipase. Life Sci. **40:**1253–1257.
33. **Kubo, M., and K. Y. Hostetler.** 1985. Mechanism of cationic amphiphilic drug inhibition of purified lysosomal phospholipase A1. Biochemistry **24:** 6515–6520.
34. **Kumar, S., and S. Srivastava.** 2005. Establishment of artemisinin combination therapy as first line treatment for combating malaria: *Artemisia annua* cultivation in India needed for providing sustainable supply chain of artemisinin. Curr. Sci. **89:**1097–1102.
35. **Lansbury, P. T., and D. M. Nowak.** 1992. An efficient partial synthesis of (+)-artemisinin and (+)-deoxoartemisinin. Tetrahedron Lett. **33:**1029–1032.
36. **Li, W., W. Mo, D. Shen, L. Sun, J. Wang, S. Lu, J. M. Gitschier, and B. Zhou.** 2005. Yeast model uncovers dual roles of mitochondria in the action of artemisinin. PLoS Genet. **1:**e36.
37. **Li, Y., and W. Y.** 2003. An over four millennium story behind qinghaosu (artemisinin)—a fantastic antimalarial drug from a traditional Chinese herb. Curr. Med. Chem. **10:**2197–2230.
38. **Lin, H. J., P. Herman, J. S. Kang, and J. R. Lakowicz.** 2001. Fluorescence lifetime characterization of novel low-pH probes. Anal. Biochem. **294:**118–125.
39. **Maeno, Y., T. Toyoshima, H. Fujioka, Y. Ito, S. R. Meshnick, A. Benakis, W. K. Milhous, and M. Aikawa.** 1993. Morphologic effects of artemisinin in *Plasmodium falciparum*. Am. J. Trop. Med. Hyg. **49:**485–491.
40. **Maerki, S., R. Brun, S. A. Charman, A. Dorn, H. Matile, and S. Wittlin.** 2006. *In vitro* assessment of the pharmacodynamic properties and the partitioning of OZ277/RBx-11160 in cultures of *Plasmodium falciparum* J. Antimicrob. Chemother. **58:**52–58.
41. **Malenga, G., A. Palmer, S. Staedke, W. Kazadi, T. Mutabingwa, E. Ansah, K. I. Barnes, and C. J. Whitty.** 2005. Antimalarial treatment with artemisinin combination therapy in Africa. BMJ **331:**706–707.
42. **Matsumoto, M., S. Dobasshi, K. Kuroda, and K. Kondo.** 1985. Sensitized photo-oxygenation of acyclic conjugated dienes. Tetrahedron **41:**2147–2154.
43. **Medicines for Malaria Venture.** 2006. Drug development and discovery projects. *In* Medicines for Malaria Venture annual report. Medicines for Malaria Venture, Geneva, Switzerland. http://www.mmv.org.
44. **Meshnick, S. R.** 2002. Artemisinin: mechanisms of action, resistance and toxicity. Int. J. Parasitol. **32:**1655–1660.
45. **Mutabingwa, T. K.** 2005. Artemisinin-based combination therapies (ACTs): best hope for malaria treatment but inaccessible to the needy! Acta Trop. **95:**305–315.
46. **Olliaro, P., F. Castelli, S. Caligaris, P. Druilhe, and G. Carosi.** 1989. Ultrastructure of *Plasmodium falciparum* "in vitro." II. Morphological patterns of different quinolines effects. Microbiologica **12:**15–28.
47. **Olliaro, P. L., R. K. Haynes, B. Meunier, and Y. Yuthavong.** 2001. Possible modes of action of the artemisinin-type compounds. Trends Parasitol. **17:** 122–126.
48. **O'Neill, P. M.** 2004. Medical chemistry: a worthy adversary for malaria. Nature **430:**838–839.
49. **Paitayatat, S., B. Tarnchompoo, Y. Thebtaranonth, and Y. Yuthavong.** 1997. Correlation of antimalarial activity of artemisinin derivatives with binding affinity with ferroprotoporphyrin IX. J. Med. Chem. **40:**633–638.
50. **Pandey, A. V., B. L. Tekwani, R. L. Singh, and V. S. Chauhan.** 1999. Artemisinin, an endoperoxide antimalarial, disrupts the hemoglobin catabolism and heme detoxification systems in malarial parasite. J. Biol. Chem. **274:** 19383–19388.
51. **Perry, C. S., S. A. Charman, R. J. Prankerd, F. C. Chiu, Y. Dong, J. L. Vennerstrom, and W. N. Charman.** 2006. Chemical kinetics and aqueous degradation pathways of a new class of synthetic ozonide antimalarials. J. Pharm. Sci. **95:**737–747.
52. **Posner, G., J. Cumming, and M. Krasavin.** 2000. Carbon-centered radicals and rational design of new antimalarial peroxide drug, p. 289–309. *In* P. F. Torrence (ed.), Biomedical chemistry: applying chemical principles to the understanding and treatment of disease. John Wiley & Sons, Inc., New York, NY.
53. **Posner, G. H., H. O'Dowd, P. Ploypradith, J. N. Cumming, S. Xie, and T. A. Shapiro.** 1998. Antimalarial cyclic peroxy ketals. J. Med. Chem. **41:**2164–2167.
54. **Posner, G. H., X. Tao, J. N. Cumming, D. Klinedinst, and T. A. Shapiro.** 1996. Antimalarially potent, easily prepared, fluorinated endoperoxides. Tetrahedron Lett. **37:**7225–7228.
55. **Posner, G. H., D. Wang, J. N. Cumming, C. H. Oh, A. N. French, A. L. Bodley, and T. A. Shapiro.** 1995. Further evidence supporting the importance of and the restrictions on a carbon-centered radical for high antimalarial activity of 1,2,4-trioxanes like artemisinin. J. Med. Chem. **38:**2273–2275.
56. **Posner, G. P., and S. R. Meshnick.** 2001. Radical mechanism of action of the artemisinin-type compounds. Trends Parasitol. **17:**266–268.
57. **Rathod, P. K., T. McErlean, and P. C. Lee.** 1997. Variations in frequencies of drug resistance in *Plasmodium falciparum*. Proc. Natl. Acad. Sci. USA **94:**9389–9393.
58. **Raynes, K., M. Foley, L. Tilley, and L. W. Deady.** 1996. Novel bisquinoline antimalarials. Synthesis, antimalarial activity, and inhibition of haem polymerisation. Biochem. Pharmacol. **52:**551–559.
59. **Ridley, R. G.** 2003. Malaria: to kill a parasite. Nature **424:**887–889.
60. **Robert, A., C. Bonduelle, S. A. Laurent, and B. Meunier.** 2006. Heme alkylation by artemisinin and trioxaquines. J. Phys. Org. Chem. **19:**562–569.
61. **Robert, A., O. Dechy-Cabaret, J. Cazelles, and B. Meunier.** 2002. From mechanistic studies on artemisinin derivatives to new modular antimalarial drugs. Acc. Chem. Res. **35:**167–174.
62. **Robinson, T. V., D. K. Taylor, and E. R. T. Tiekink.** 2006. Osmium catalyzed dihydroxylation of 1,2-dioxines: a new entry for stereoselective sugar synthesis. J. Org. Chem. **71:**7236–7244.
63. **Rosenthal, P. J., J. H. McKerrow, M. Aikawa, H. Nagasawa, and J. H. Leech.** 1988. A malarial cysteine proteinase is necessary for hemoglobin degradation by *Plasmodium falciparum*. J. Clin. Investig. **82:**1560–1566.
64. **Tang, Y., Y. Dong, and J. L. Vennerstrom.** 2004. Synthetic peroxides as antimalarials. Med. Res. Rev. **24:**425–448.
65. **Taylor, D. K., T. D. Avery, B. W. Greatrex, E. R. Tiekink, I. G. Macreadie, P. I. Macreadie, A. D. Humphries, M. Kalkanidis, E. N. Fox, N. Klonis, and L. Tilley.** 2004. Novel endoperoxide antimalarials: synthesis, heme binding, and antimalarial activity. J. Med. Chem. **47:**1833–1839.
66. **Tilley, L., T. Davis, and P. Bray.** 2006. Prospects for treatment of drug-resistant malaria parasites. Future Microbiol. **1:**127–141.
67. **Turner, J. A., and W. Herz.** 1977. Unusual effect of epoxidic oxygen on the ease of base-catalyzed decomposition of epidioxides. J. Org. Chem. **42:**2006–2008.
68. **Uhlemann, A. C., A. Cameron, U. Eckstein-Ludwig, J. Fischbarg, P. Iserovich, F. A. Zuniga, M. East, A. Lee, L. Brady, R. K. Haynes, and S. Krishna.** 2005. A single amino acid residue can determine the sensitivity of SERCAs to artemisinins. Nat. Struct. Mol. Biol. **12:**628–629.
69. **Uhlemann, A. C., S. Wittlin, H. Matile, L. Y. Bustamante, and S. Krishna.** 2007. Mechanism of antimalarial action of the synthetic trioxolane RBX11160 (OZ277). Antimicrob. Agents Chemother. **51:**667–672.
70. **Vennerstrom, J. L., S. Arbe-Barnes, R. Brun, S. A. Charman, F. C. K. Chiu, J. Chollet, Y. Dong, A. Dorn, D. Hunziker, H. Matile, K. McIntosh, M. Padmanilayam, J. Santo Tomas, C. Scheurer, B. Scorneaux, Y. Tang, H. Urwyler, S. Wittlin, and W. N. Charman.** 2004. Identification of an antimalarial synthetic trioxolane drug development candidate. Nature **430:**900–904.
71. **Whitty, C. J., R. Allan, V. Wiseman, S. Ochola, M. V. Nakyanzi-Mugisha, B. Vonhm, M. Mwita, C. Miaka, A. Oloo, Z. Premji, C. Burgess, and T. K. Mutabingwa.** 2004. Averting a malaria disaster in Africa—where does the buck stop? Bull. W. H. O. **82:**381–384.
72. **Wissing, F., C. P. Sanchez, P. Rohrbach, S. Ricken, and M. Lanzer.** 2002. Illumination of the malaria parasite *Plasmodium falciparum* alters intracellular pH. Implications for live cell imaging. J. Biol. Chem. **277:**37747–37755.
73. **Yayon, A., R. Timberg, S. Friedman, and H. Ginsburg.** 1984. Effects of chloroquine on the feeding mechanism of the intraerythrocytic human malarial parasite *Plasmodium falciparum*. J. Protozool. **31:**367–372.
74. **Yeung, S., W. Pongtavornpinyo, I. M. Hastings, A. J. Mills, and N. J. White.** 2004. Antimalarial drug resistance, artemisinin-based combination therapy, and the contribution of modeling to elucidating policy choices. Am. J. Trop. Med. Hyg. **71:**179–186.